Estimates of cluster-impact fusion yields

C. Carraro, B. Q. Chen, S. Schramm, and S. E. Koonin
W. K. Kellogg Radiation Laboratory, California Institute of Technology, Pasadena, California 91125
(Received 15 January 1990)

We present several theoretical estimates of D+D fusion rates for heavy-water molecular clusters impacting on TiD targets. Our considerations range from the simple thick-target yield to single- and multiple-deuteron knock-on to thermonuclear and thermal-spike models; detailed molecular-dynamics simulations are also presented. Each of our models fails, by many orders of magnitude, to reproduce the yields observed in recent experiments. We consider the extent to which experimental artifacts might contribute to the results claimed.

I. INTRODUCTION

The work reported in this paper was stimulated by recent claims to have observed D+D fusion products when heavy-water molecular cluster ions impact a titanium deuteride target.[1] For $(D_2O)_N$ clusters with a fixed total energy of 300 keV, the yield (fusions per impact) shows a modest peak near $N=200$, but remains roughly constant at some 10^{-12}–10^{-11} as N varies from 20 to 1000. (See Fig. 1.) A related study of the energy dependence of the yield for fixed $N=150$ showed an increase of yield with increasing energy less rapid than would be expected. In later work,[2] fusion was detected when light water clusters bombarded deuterated targets (albeit at only 5% of the heavy-water rate) any yields several times those obtained with TiD targets were observed using deuterated polyethylene targets.

There can be no doubt that fusion has been observed in the experiments described above; the detection of protons and ^{3}H with the correct energy is unambiguous. However, it is a puzzle that any fusion occurs at all, given the very low energies per incident deuteron involved in these experiments. Moreover, the essential constancy of the yield as the energy per deuteron drops by a factor of 50 is equally puzzling, given that the elementary D+D fusion cross section drops by over 90 orders of magnitude. Clearly, some exotic explanation is required if the experiments are correct. For example, the authors of Ref. 1

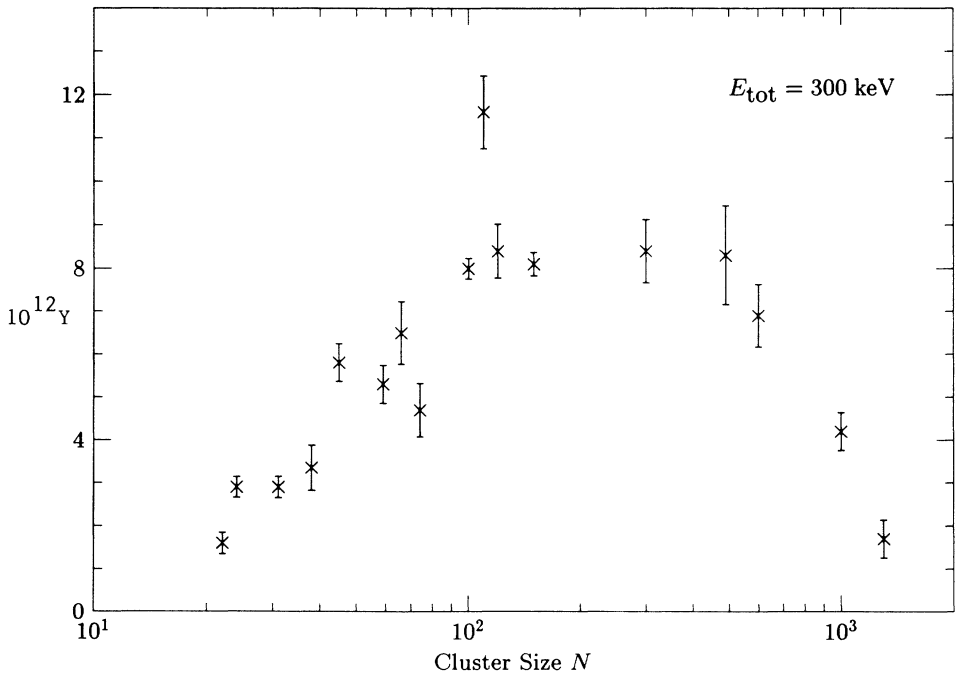

FIG. 1. Total fusion yield per cluster as a function of cluster size at a total energy of 300 keV (taken from Fig. 3 of Ref. 1). We have converted the proton counts to total fusion yield per cluster normalizing to the fusion rate value of 0.05 sec^{-1} per cluster nA of $(D_2O)_{100}$ reported in Ref. 1.

suggest that the D+D fusion rate might be enhanced through compression of the target by the impacting cluster.

Our purpose in this paper is to assess these results in light of our current understanding of the nuclear and atomic physics involved in D+D fusion during cluster impact. We show below that each of a variety of analytic models describing the early, intermediate, and late stages of the impact fails to reproduce the experimental observations by many orders of magnitude. Further, we have analyzed molecular-dynamics simulations of heavy-water clusters impacting on heavy water and fail to find any evidence for exotic phenomena of the kind required. We therefore conclude that the observations cannot be accommodated within a conventional framework. However, we have also considered whether experimental artifacts could contribute to the observed fusion yields and conclude that this is within the realm of possibility. Clearly, further experimental studies are required to clarify the situation.

The balance of our paper is organized as follows. In Sec. II, we present our analytical models for fusion during cluster impact and compare the results of each with the experimental data. In Sec. III, we exploit these models to consider the question of experimental artifacts. Finally, in Sec. IV, we present and analyze results from molecular-dynamics simulations of cluster impact.

II. CLUSTER FUSION YIELDS

In this section, we present simple estimates of the fusion yield from several different processes leading to D+D fusion that might occur when a heavy-water cluster impinges on a TiD target. These are important to quantify the range of possible physical effects and to provide a context in which to analyze the results of the molecular-dynamics simulations presented in Sec. IV. Throughout, we assume an amorphous TiD target. This assumption greatly simplifies both the theoretical and the numerical treatment of the problem. It is also likely a more appropriate description of the surface layers of the target during extended bombardment. Molecular-dynamics simulations of cluster bombardment of crystalline and amorphous metallic targets indicate that crystal structure is irrelevant to the process that we are investigating.[3]

A. Thick-target yield

Consider a deuteron freed by the dissociation of a cluster molecule as it strikes the target. If $E_{\rm tot}$ is the cluster energy and N the number of molecule in the cluster, then the initial kinetic energy of the deuteron is

$$E_{\rm in}=(E_{\rm tot}/N)m_{\rm D}/(2m_{\rm D}+m_{\rm O})=0.1E_{\rm tot}/N\ ,$$

where $m_{\rm D}$ and $m_{\rm O}$ are the atomic masses of the deuteron and oxygen, respectively.

The thick-target yield $Y_{\rm TT}$ (i.e., the probability that the deuteron undergoes a fusion reaction while slowing down in the target) is given by

$$Y(E_{\rm in})=\int dx\, n_{\rm D}\sigma_f(E)$$
$$=n_{\rm D}\int_0^{E_{\rm in}} dE_{\rm lab}\frac{1}{|dE_{\rm lab}/dx|}\sigma_f(E_{\rm c.m.})\ , \quad (1)$$

where $n_{\rm D}$ is the number density of deuterons in the target, σ_f is the fusion cross section, $E_{\rm c.m.}=E_{\rm lab}/2$ is the center-of-mass energy for D+D collisions, and $dE_{\rm lab}/dx$ is the stopping power for D in TiD.

The fusion cross section can be written in terms of the astrophysical S factor, $S(E)$, as[4]

$$\sigma_f(E)=\frac{S(E)}{E}\exp(-b/\sqrt{E})\ . \quad (2)$$

For the D+D reaction,[5]

$$S(E)\simeq S(0)=1.1\times10^{-22}\ \text{keV cm}^2$$

(the sum of the pT and the n ^{3}He channels) and we can ignore a slow, monotonic increase of $S(E)$ with energy.[6] The constant in the exponent is $b=31.28\ \text{keV}^{1/2}$.

The stopping power in the energy regions of interest here (and in all cases below, unless noted explicitly otherwise) is dominated by the "nuclear" contribution and is given by[7]

$$\frac{dE_{\rm lab}}{dx}=3.43\times10^{-15}n_{\rm Ti}E_{\rm lab}^{1/2}\ \text{eV cm}^2 \quad (3a)$$

for D in Ti and

$$\frac{dE_{\rm lab}}{dx}=0.89\times10^{-15}n_{\rm D}E_{\rm lab}^{1/2}\ \text{eV cm}^2 \quad (3b)$$

for D in D. Adding these two contributions gives

$$\frac{dE_{\rm lab}}{dx}=2.46\times10^{5}E_{\rm lab}^{1/2}\ \text{keV/cm} \quad (3c)$$

for $n_{\rm D}=n_{\rm Ti}=5.7\times10^{22}\ \text{cm}^{-3}$. In these expressions, $E_{\rm lab}$ is given in keV.

With the parametrizations (2) and (3c), the energy integration in Eq. (1) is elementary and we obtain

$$Y(E_{\rm in})=2.3\times10^{-6}\exp(-44.24/\sqrt{E_{\rm in}})\ , \quad (4)$$

where $E_{\rm in}$ is given in keV. Finally, we multiply by the total number of deuterons in the cluster to get the total fusion yield per cluster

$$Y_{\rm TT}=4.6\times10^{-6}N\exp(-140\sqrt{N/E_{\rm tot}}) \quad (5a)$$

and, for $E_{\rm tot}=300$ keV

$$Y_{\rm TT}=4.6\times10^{-6}N\exp(-8.077\sqrt{N})\ . \quad (5b)$$

This yield is plotted in Fig. 2 as a function of N, together with the predictions of the other models we discuss below and the experimental data, as presented in Fig. 1.

B. Deuteron knock-on

We now consider the process in which an oxygen atom from the incident water cluster molecule scatters elastically from a deuteron at rest in the TiD lattice, transferring energy U. This process might be important as it re-

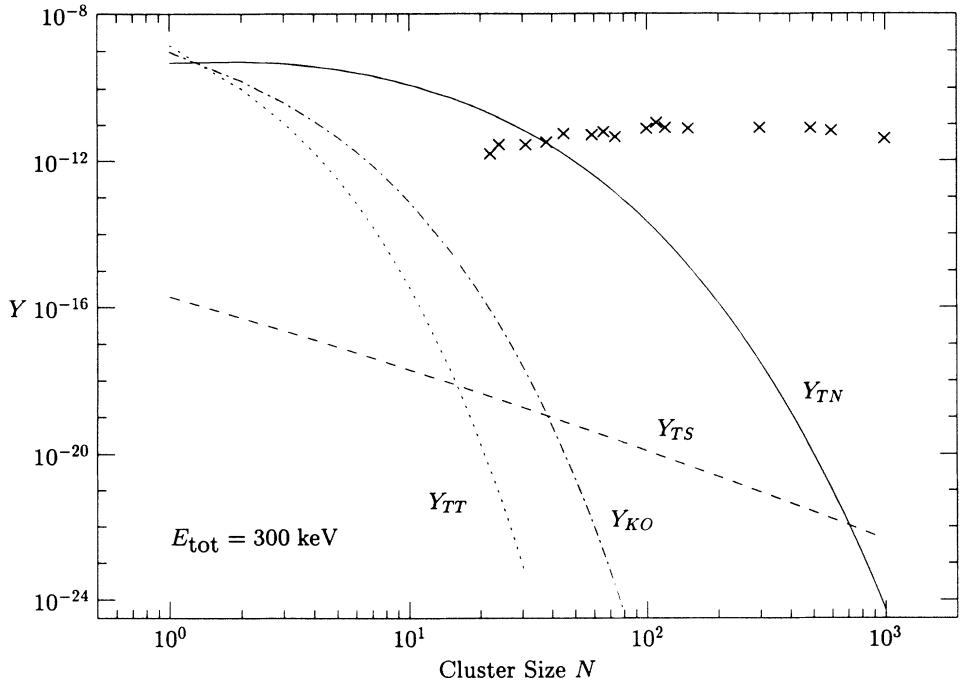

FIG. 2. Total fusion yield per cluster as a function of cluster size at a total energy of 300 keV. Note the logarithmic vertical scale. The dotted curve is the thick-target fusion yield for the incident heavy-water deuterons. The dash-dotted curve considers substrate deuteron knock-on by incident heavy-water oxygens. The solid curve assumes thermalization of the atomic degrees of freedom upon impact. The dashed curve is the yield predicted by a thermal-spike model of the collision cascade. The experimental points are taken from Fig. 3 of Ref. 1 and normalized as described for Fig. 1.

sults in deuterons with kinetic energies greater than those that come from the heavy-water cluster directly. Indeed, the kinetic energy of an oxygen atom from the cluster is $E_0=0.8E_{\rm tot}/N$ and the maximum energy that it can transfer to a stationary deuteron is $U_{\rm max}=0.395E_0$; the energy of D atoms in a cluster molecule is only $0.125E_0$. Accounting for the slowing of the oxygen atom in the target, the fusion yield of the knocked-on deuterons is

$$Y_{\rm KO}=n_{\rm D}N\int_0^{E_0}dE\frac{1}{|dE/dx|}\times\int_0^{U_{\rm max}(E)}dU\,Y(U)\frac{d\sigma(U,E)}{dU}\ , \qquad (6)$$

where $d\sigma/dU$ is the differential energy-transfer cross section for O-D collisions, and $Y(U)$ is the thick-target yield per deuteron given by Eq. (4). Using the appropriate universal cross-section parametrization,[8] we find

$$\frac{d\sigma(U,E)}{dU}=\sigma_0U^{-4/3}E^{-1/3}\ , \qquad (7)$$

where $\sigma_0=2.2\times10^{-17}$ yields the cross section in cm^2 if U and E are expressed in keV. The stopping power for oxygen in TiD calculated from universal stopping cross sections[8] is

$$dE/dx\simeq3.5\times10^6[E^{1/2}({\rm keV})]{\rm keV/cm}\ .$$

In contrast to Eq. (1), the energy integration in Eq. (6) is nontrivial, but sufficient accuracy can be achieved with asymptotic expansions to leading order. Thus, the total fusion yield from the knock-on mechanism is

$$Y_{\rm KO}=7.5\times10^{-10}E_{\rm tot}^{5/6}N^{1/6}\exp(-78.7\sqrt{N/E_{\rm tot}}) \qquad (8)$$

and, at a cluster energy of 300 keV,

$$Y_{\rm KO}=8.7\times10^{-8}N^{1/6}\exp(-4.54\sqrt{N})\ . \qquad (9)$$

It should be noted that the use of a cross-section parametrization different from that given by Eq. (7) would lead to slightly different prefactors in Eq. (9). However, the order of magnitude of the yield, dominated by the energy exponential, is unchanged in the range of energies pertinent to the experiment. For small clusters ($N\lesssim5$), the deficiencies of the parametrization (7) cause Eq. (9) to overestimate the knock-on yield by about an order of magnitude.

C. Multiple knock-on

Multiple knock-on processes achieve even higher deuteron energies (and hence higher fusion yields) than the single knock-on process discussed above. After a target deuteron is knocked on by an incoming oxygen, it could backscatter by a target titanium atom and then be further accelerated by colliding with another (or even the same) incoming oxygen atom. This process, analogous to the Fermi mechanism for accelerating cosmic rays,[9] seems very unlikely as multiple nearly head-on collisions are required to transfer a substantial energy to the deuteron. However, it cannot be discarded *a priori* since the D+D fusion yield depends strongly on the deuteron en-

ergy; even rare high-energy deuterons could significantly increase the fusion yield.

Since we will discuss results of a full numerical treatment of cluster impact in Sec. IV, we restrict ourselves here to upper estimates of the yield from multiple knock-on processes. Thus, we assume that *every* knock-on process is followed by a second one in the manner as described above. In the case where a deuteron of energy U backscatters from a titanium atom and then again from the oxygen, the final energy $\tilde{U}$ of the deuteron is

$$\frac{\tilde{U}}{U}=\left[\frac{M_O-M_D}{M_O+M_D}\frac{2M_{Ti}}{M_{Ti}+M_D}\right]^2\approx 2.23 . \tag{10}$$

Within the approximations stated above, the fusion yield of the double-knock-on (DKO) process can then be determined directly from Eq. (6) by replacing $Y(U)$ with $Y(\tilde{U})$, giving

$$Y_{DKO}=8.7\times 10^{-8}N^{1/6}\exp(-3.04\sqrt{N}) , \tag{11}$$

which differs from the knock-on yield (8) by the constant in the exponential.

To obtain an even less restrictive upper bound on multiple knock-ons (MKO's) we can assume that *every* oxygen atom transfers *all* of its energy to a deuteron in the target through multiple backscatterings. Since every oxygen in the initial $(D_2O)_N$ cluster has energy $E_O=0.8E_{tot}/N$, this results in N deuterons, each with energy E_O. Further assuming that this condition occurs in *every* impact, the fusion yield can be directly calculated from Eq. (4) as

$$Y_{MKO}=2.3\times 10^{-6}N\exp(-2.86\sqrt{N}) . \tag{12}$$

Even for the extremely optimistic assumptions behind these estimates, the calculated fusion yield cannot explain the rough constancy of the experimental data at large N as the calculated yield for $N\sim 1000$ drops by more than 30 orders of magnitude with respect to the $N=25$ value.

D. Thermonuclear model

A model at the opposite extreme from the "preequilibrium" processes we have considered thus far arises from assuming that the incident cluster thermalizes in the TiD and produces a hot gas of atoms. This gas will expand and cool as it involves more atoms in the solid. We take the total energy of the expanding gas to be constant, $VT=V_0T_0$, where V and T are the volume and temperature, and the zero subscript refers to the initial values. If we assume that the cluster thermalizes with an equal number of the target molecules, then $5(3/2T_0)=E_{tot}/N$ (the factor 5 accounts for one Ti, one O, and three D nuclei), and $V_0=N/n_{D_2O}$ is the initial volume of the plasma. Note that throughout we neglect the electronic degrees of freedom as the relatively slow nuclear motion couples to them on a time scale much longer than that relevant here.

The rate of D+D reactions per unit volume is given by[4]

$$R(T)=7.20\times 10^5 n_D^2 S_0(\text{keV cm}^2)\tau^2\exp(-\tau) , \tag{13}$$

where $\tau=42.48/T_6^{1/3}$ and T_6 is the temperature of the gas in 10^6 K. The total number of fusions in the impact is given by the space-time integral of the fusion rate

$$Y_{TN}=\int_0^{T_0}dT\frac{1}{|\dot{T}|}V(T)R(T) . \tag{14}$$

The cooling rate, $\dot{T}$, is related to the expansion rate as

$$\dot{T}=-(T/V)\dot{V}=-3Tc(T)/V^{1/3} ,$$

where the expansion velocity $c(T)=\sqrt{3T/m_{Ti}}$ can be taken to be the thermal velocity at temperature T in the target. Performing the integral Eq. (14), we find

$$Y_{TN}=1.4\times 10^{-5}E_{tot}^{-5/6}N^{13/6}\exp\left[-36.7\left[\frac{N}{E_{tot}}\right]^{1/3}\right] , \tag{15a}$$

where E_{tot} is measured in keV; for $E_{tot}=300$ keV, we obtain

$$Y_{TN}=1.2\times 10^{-7}N^{13/6}\exp(-5.49N^{1/3}) . \tag{15b}$$

The calculation assumes a hot gas in free expansion, with a time scale $\sim V_0^{1/3}/c(T)$; this is 10^{-14}–10^{-13} sec for clusters of a few hundred molecules. A more refined estimate of the confinement time must consider that expansion occurs within the cold solid. A fluid-dynamic calculation shows that the effect of such "tamping" is to increase the confinement time by about a factor of 3,[10] which still falls some 10^{12} orders of magnitude short of explaining the yields reported in Ref. 1.

We have neglected any effect of electronic screening in our estimate of the thermonuclear rate. Screening enhancements are of the form $\exp(U/T)$, where U is a typical electronic energy ≈ 10 eV. As the most important values of T are close to $T_0\approx 100$'s of eV, such an enhancement is negligible.

E. Thermal-spike model

Next, we lift the assumption that the cluster equilibrates with an equal number of target molecules. Instead, we assume that the energy is deposited in a small cylinder, coaxial with the path of the cluster through the target; this is often called a thermal spike.[11] As we show below, this model emphasizes the energy deposition in the first atomic layers of the solid, leading to a rather weak N dependence of the temperature.

Consider the usual thermal-spike (TS) model,[11] where energy is deposited in a volume $dV=\Sigma dx$ as the fast atoms from the impinging cluster move a distance dx into the target. A lower bound on Σ is the cross section of the cluster

$$\Sigma=\pi\left[\frac{3N}{4\pi n_{D_2O}}\right]^{2/3} . \tag{16}$$

The target deuterons in a small cylinder, at a depth x from the surface, are supposed to thermalize at a temperature given by the relation

$$\tfrac{3}{2}n_{\text{target}}T(x)=\frac{1}{\Sigma}\frac{N\,dE(x)}{dx}\ . \tag{17}$$

Here $dE(x)/dx$ denotes the energy lost by each water molecule to the atoms in the target (by far the main contribution coming from the oxygen atoms). Using again universal parametrizations,[8] we have

$$dE(x)/dx=4\times10^{6}E(x)^{1/2}\ \text{keV cm}^{-1}\ ,$$

where $E(x)$ is the projectile energy in keV at a depth x. For fixed E_{tot}, E scales as $1/N$, yielding

$$T(x=0)\simeq2.0\times10^{-2}E_{\text{tot}}^{1/2}N^{-1/6}\ \text{keV}\ . \tag{18}$$

Comparisons to the value $T_0=0.133E_{\text{tot}}/N$ used in our thermonuclear model show that N dependence is much weaker in the thermal-spike model but the characteristic temperatures involved are smaller.

The total yield is given by the space-time integral of the thermonuclear rate over the spike region,

$$\begin{aligned}Y_{\text{TS}}&\equiv\int_0^{\infty}dx\,\Sigma dt\,R(T(x,t))\\&=\int_0^{E_0}dE\frac{1}{|dE/dx|}\int_0^{T(E)}dT\frac{\Sigma}{|\dot{T}|}R(T)\ .\end{aligned} \tag{19}$$

One can now proceed to model the expansion as for Y_{TN}, taking the total energy per unit length along the path to be constant, $\Sigma T=\Sigma_0T_0$. The different geometry and the weak dependence of the temperature on cluster size affect the overall prefactor as well as the energy exponential, leading to

$$Y_{\text{TS}}=1.6\times10^{-5}E_{\text{tot}}^{1/4}N^{-5/12}\exp(-68.9N^{1/18}E_{\text{tot}}^{-1/6}) \tag{20a}$$

and, for $E_{\text{tot}}=300$ keV,

$$Y_{\text{TS}}=7\times10^{-5}N^{-5/12}\exp(-26.6N^{1/18})\ . \tag{20b}$$

This cluster-size dependence is much weaker than our previous models and the yield drops by "only" some four orders of magnitude over the experimental range of N. However, it is achieved by the extreme assumption of complete thermal isolation of the various segments along the path. Further, the absolute value of the yield is about ten orders of magnitude below the data.

F. Validity of thermal equilibrium

In a thermal model, high fusion rates can result from the collision of two deuterons in the tail of the Boltzmann distribution. Indeed, the yield is dominated by the energies close to the "Gamow peak," i.e., $E\sim E_G\equiv1.22T_6^{2/3}$ keV. We find

$$E_G=1.63(E_{\text{tot}}/N)^{2/3}\ \text{keV}$$

for the thermonuclear model and

$$E_G=0.27(E_{\text{tot}}/N^{1/3})^{1/3}\ \text{keV}$$

for the thermal-spike model at $x=0$, where E_{tot} is in keV. For $E_{\text{tot}}=300$ keV and $N=100$, this results in $E_G=3.4$ and 1.1 keV, respectively. The maximum energy that can be imparted to a deuteron in a single collision (by an incident oxygen) is about 1 keV. Thus, such a collision can produce deuterons at the Gamow energy; however, it is extremely unlikely to occur, with a typical mean free path of several hundred lattice spacings.

We can legitimately ask whether a different energy distribution can explain the observed yields. For example, a power-law energy spectrum for the random collision cascades in the target $p(E)\propto E^{-m}$, was suggested by Thompson.[12] It is interesting to note that such a spectrum leads to a nonexponential dependence of the fusion yield upon the cluster size N at fixed E_{tot} (or upon the incident energy at fixed N), since a power-law spectrum has no characteristic scale. We can derive this result by a saddle-point evaluation of the rate integral

$$\int d^3v_1d^3v_2\sigma(|v_1-v_2|)|v_1-v_2|f(v_1)f(v_2)\ , \tag{21}$$

where the velocity distribution is given by

$$f(v)=p(E)/v\sim v^{-(2m+1)}$$

and the cross section is given by Eq. (2). Simple dimensional analysis yields the saddle-point equation

$$\frac{d}{dv}(-b/v-2m\ln v)=0\ , \tag{22}$$

and hence the most effective energy, E_0, is given by

$$E_0=b^2/4m^2=245/m^2\ \text{keV}\ , \tag{23}$$

independent of the incident energy. Of course, the initial energy of the cascade must satisfy

$$E_{\text{in}}\gg245/m^2\ \text{keV} \tag{24}$$

to justify a saddle-point analysis. Since in the experiment $E_{\text{in}}<3$ keV for $N<100$, this requires $m\gg10$, while experiments and computer simulations[13] strongly support $m\simeq2$. Under these circumstances, the rate integral (21) is best evaluated by asymptotic expansions, and the results behave much like the knock-on yield (see dash-dotted curve of Fig. 2). This is as expected, since the energy cascade is initiated by knock-on processes.

We have presented in this section simple models for a variety of mechanisms resulting in D+D fusion during cluster impact. These range from nonequilibrium processes occurring early in the impact, to the partial equilibrium of the thermal spike, to the full equilibrium of the thermonuclear model. None of these can account for both the magnitude and N dependence of the experimental data at fixed $E_{\text{tot}}=300$ keV; the shortfall in all cases is many orders of magnitude. Unexpected cooperative effects that can enhance the rates by ten or twenty orders of magnitude are, of course, still possible. However, our multiple knock-on, thermonuclear, thermal-spike, and collision cascade models all account, in different ways and degrees, for some cooperative effect. The occurrence of some new, unexpected phenomenon is most convincingly tested by molecular-dynamics simulations, as we describe in Sec. IV. However, in the next section, we exploit the analytical estimates presented above to explore

the possibility that experimental artifacts are responsible for the observed rates.

III. EXPERIMENTAL CONSIDERATIONS

Our discussion of the various models in Sec. II shows that the salient feature of the data is the near N independence of the fusion yield. For fixed $E_{\rm tot}=300$ keV, the experimental yield varies by only about an order of magnitude as N varies from 20 to 1000. Our "best effort" was the thermonuclear model, which could explain the fusion yield for one specific cluster size ($N\sim 40$) but could not reproduce the constancy of the data, especially for large cluster sizes. The rapid N dependence of all of our models is, of course, due to the rapid energy dependence of the elementary D+D cross section.

A. Contamination by light fragments

A natural explanation of an approximately N-independent fusion yield is the contamination of the beam with some fraction of smaller, higher-velocity clusters (or even single deuterons). Since the mass spectrometer in the experiments[1] is placed before the accelerator, collisions of the $(D_2O)_N$ cluster with the residual gas molecules in the accelerator column can split off a small charged cluster that would be accelerated to much higher velocities than the original cluster. For instance, a pressure of 10^{-7}–10^{-6} Torr corresponds to a mean free path of 10^5–10^6 cm and for an accelerator length of some 10^2 cm, there will be a small, but non-negligible, amount of lighter clusters produced. Experimentally,[1,2] the possibility of small high-energy clusters was investigated directly by detecting the accelerated particles with a silicon detector shielded by an Al film to stop large clusters. From these measurements, upper limits were derived for the fractions f of high-energy D_2O and D in the beam: $f_{D_2O}<2\times 10^{-4}$ and $f_D<10^{-5}$.

To estimate the effect of high-energy D_2O and D in the beam, we adopt the thick-target calculations of Sec. II A. Since a fully accelerated single deuteron has an energy of 300 keV, we must use a parametrization of the stopping power that is valid over a broader range of energies than that of Eq. (3) (i.e., we must include the electronic stopping power). Thus, from Ref. 5, we take

$$
\begin{aligned}
&dE_{\rm lab}dx = A_0\times 10^5 E_{\rm lab}^{1/2}\ \text{keV/cm},\quad E_{\rm lab}<20\ \text{keV}\ ,\\
&\left[\frac{dE_{\rm lab}}{dx}\right]^{-1}=\left[\frac{dE_{\rm lab}}{dx}\right]_1^{-1}+\left[\frac{dE_{\rm lab}}{dx}\right]_2^{-1}\ ,\\
&\qquad\qquad E_{\rm lab}\geq 20\ \text{keV}\ ,\\
&\left[\frac{dE_{\rm lab}}{dx}\right]_1 = A_1 E_{\rm lab}^{0.45}\ \text{keV/cm}\ ,\\
&\left[\frac{dE_{\rm lab}}{dx}\right]_2 = \frac{A_2}{E_{\rm lab}}\ln(1+A_3/E_{\rm lab}+A_4E_{\rm lab})\ \text{keV/cm}.
\end{aligned}
\tag{25}
$$

The parameters (A_0,A_1,A_2,A_3,A_4) are $(5.03\times 10^4, 5.98\times 10^4, 2.77\times 10^7, 2.4\times 10^4, 0.0577)$ for deuterium and $(1.96\times 10^5, 2.29\times 10^5, 5.90\times 10^8, 1143, 0.0047)$ for titanium, respectively. Numerical integration of Eq. (1) with the stopping power Eq. (25) results in thick-target fusion yields for a 300-keV deuteron and a 300-keV D_2O molecule of $Y(D)=2.9\times 10^{-7}$ and $Y(D_2O)=1.5\times 10^{-9}$. Thus, fractions of high-energy D or D_2O $f_D\sim 2\times 10^{-5}$ or $f_{D_2O}\sim 5\times 10^{-3}$ would be sufficient to produce the experimental values. In view of the experimental limits quoted above, the Al-film experiment cannot convincingly exclude contamination of the beam with high-energy deuterons as an explanation of the measured yields.

A further experimental investigation of possible beam contamination has been performed by covering the target with a gold foil. Two thicknesses of the foil were used, $t_1=100\ \mu\text{g/cm}^2$ and $t_2=500\ \mu\text{g/cm}^2$. Preliminary results[2] show that the measured fusion yield is at least a factor of 10 smaller in the case of t_2 relative to t_1. This result can be used to derive an upper estimate for the particle energy of a possible D contamination. The energy loss of a deuterium ion in the foil can be computed with the help of Eq. (25); the stopping-power parameters for a gold target are[7] $(2.03\times 10^5, 2.36\times 10^5, 2.17\times 10^9, 877, 1.3\times 10^{-3})$. The thick-target fusion yield is then determined as described above, but using the energy of the deuterium as it exits the foil. Assuming that the yield decreases at least by a factor of 10 as the foil thickness increases from t_1 to t_2, one finds $E(D)<50$ keV or $E(D_2O)<500$ keV. These results obviously give no further information on single D_2O contamination. However, the thick-target fusion yield of 50-keV deuterons is $Y\sim 4.6\times 10^{-9}$, so that an explanation of the experimental data requires a contamination $f_D\sim 10^{-3}$; this exceeds the experimental upper limit by about two orders of magnitude.

Further information on single D_2O contamination is provided by the results with light-water clusters. Our discussion of knock-on yields (Sec. II B) reveals that, at cluster number $N=1$, the knock-on yield falls about an order of magnitude below the thick-target yield. Hence, for single water-molecule impacts, we expect the H_2O yield to be $\lesssim 0.1$ times the D_2O yield, which is consistent with experiment.

Reference 1 presented a preliminary study of the beam-energy dependence of the D+D fusion yields, for fixed cluster size, $N=150$. The results showed that the fusion yield decreased by about one order of magnitude as the beam energy decreased from 300 to 225 keV. Again using Eq. (1) we can determine the D or D_2O energy that would reproduce this energy dependence (i.e., that shows a decrease of the fusion rate by a factor of 10 for 25% decrease of the initial energy). The resulting values are

$$
\begin{aligned}
&E_D\approx 9\ \text{keV},\quad Y=8.6\times 10^{-13}\ ,\\
&E_{D_2O}\approx 90\ \text{keV},\quad Y=1.7\times 10^{-12}
\end{aligned}
$$

which are large enough to agree with the data but are in conflict with the assumption of small high-velocity debris

as source of the observed fusion processes (i.e., they would require the unreasonable assumption $f_{D,D_2O} \sim 1$).

B. Effects of mass dispersion

The models discussed in the previous section have idealized the true experimental conditions by assuming that the incident cluster beam had a "monochromatic" mass spectrum. Because lighter clusters have a higher velocity (and hence a higher fusion yield), there are corrections to our predicted yields due to the known (experimentally measured) mass dispersion at the quadrupole mass analyzer.

The mass spectrum of the beam, as selected by the quadrupole analyzer, shows a dispersion of N about its nominal value, N_0. The experiments[2] had a FWHM of αN_0, with $\alpha \simeq 0.4$, and strictly excluded $N < N_0/2$ at the low-energy end of the accelerator. Assuming that no fragments are accelerated with $N < N_0/2$, we have investigated the effects of both Gaussian and Lorentzian mass distributions on the yields predicted by our models. The results, displayed in Fig. 3 (dashed lines) for Gaussian distribution, show, at best, a two-order-of-magnitude increase over the case of a single-mass beam for Y_{TN}, and an even more irrelevant enhancement of Y_{TT}.

A much more dramatic increase of the yield is achieved by removing the restriction $N > N_0/2$. Such a distribution would better reproduce the actual experimental conditions if some amount of cluster breakup occurred during the acceleration. By folding the thick-target and thermonuclear yields with the cluster-size distribution

$$P_{N_0}(N) \propto \exp[-(N-N_0)^2/2N_0^2\alpha^2] , \tag{26}$$

we can reproduce the order of magnitude of the observed yields with the rather large value of $\alpha = 0.5$ (Fig. 3, dash-dotted lines). A Lorentzian N distribution with the experimental FWHM, $0.4N_0$, would also reproduce the data. In contrast, the resulting Y_{TN} shows a much weaker energy dependence than the data (see Fig. 4 of Ref. 1; note that two experimental proton counts are reported for a 300-keV $N = 150$ cluster in Fig. 3 and Fig. 4 of Ref. 1, and that they differ by a factor of 2). However, the thick-target yield Y_{TT} does reproduce the experimental trend, but accounts for only 20% of the signal (Fig. 4). We also mention here a private communication[2] showing a much more rapid dropoff of fusion rate with cluster size when the experimental mass dispersion was decreased.

Clearly, mass analysis of the projectiles after acceleration would clarify the possible effect of beam contamination.

IV. MOLECULAR-DYNAMICS SIMULATION

Our physical intuition, as embodied in the models of Sec. II, is far from exhaustive, and it is always possible that some exotic, cooperative effect comes in to play during the impact of a cluster to boost the fusion rate significantly above our expectations. To investigate such a possibility, we have performed and analyzed molecular-dynamics simulations of the impact of heavy-water clusters on heavy-water targets. Throughout, our goal is not to do a physically exact simulation, but rather to search qualitatively for processes that could explain

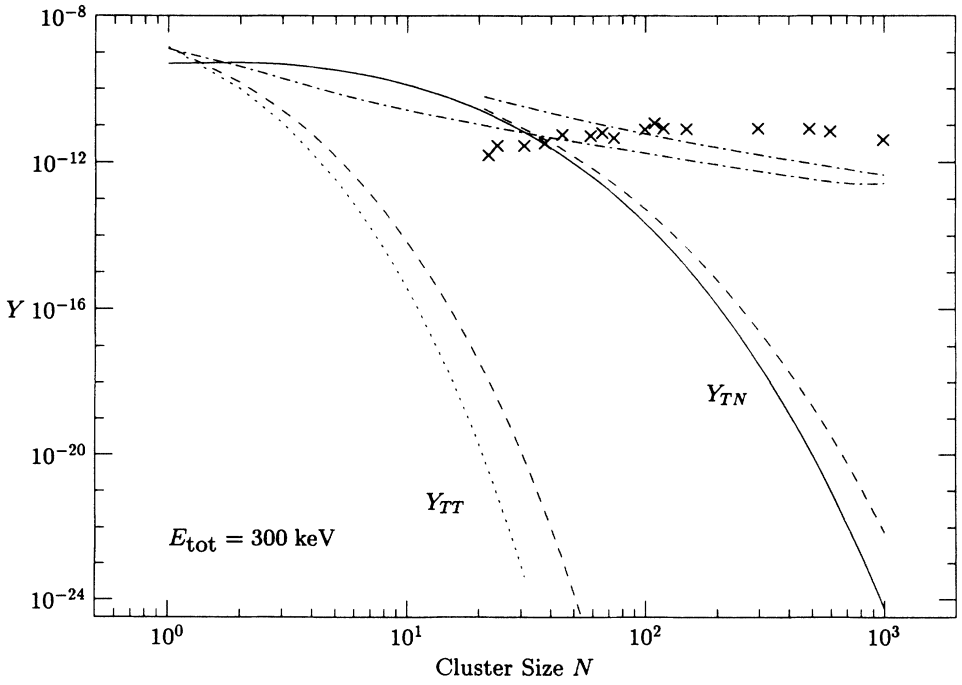

FIG. 3. Effects of mass dispersion of the beam, at a total energy of 300 keV. The dashed curves are obtained by folding Y_{TT} and Y_{TN} with a Gaussian dispersion [Eq. (26)], with $\alpha = 0.2$. We have applied a cut, $N > N_0/2$. The dash-dotted curves are obtained by folding Y_{TT} and Y_{TN} with a Gaussian dispersion [Eq. (26)] with $\alpha = 0.5$ and no cut.

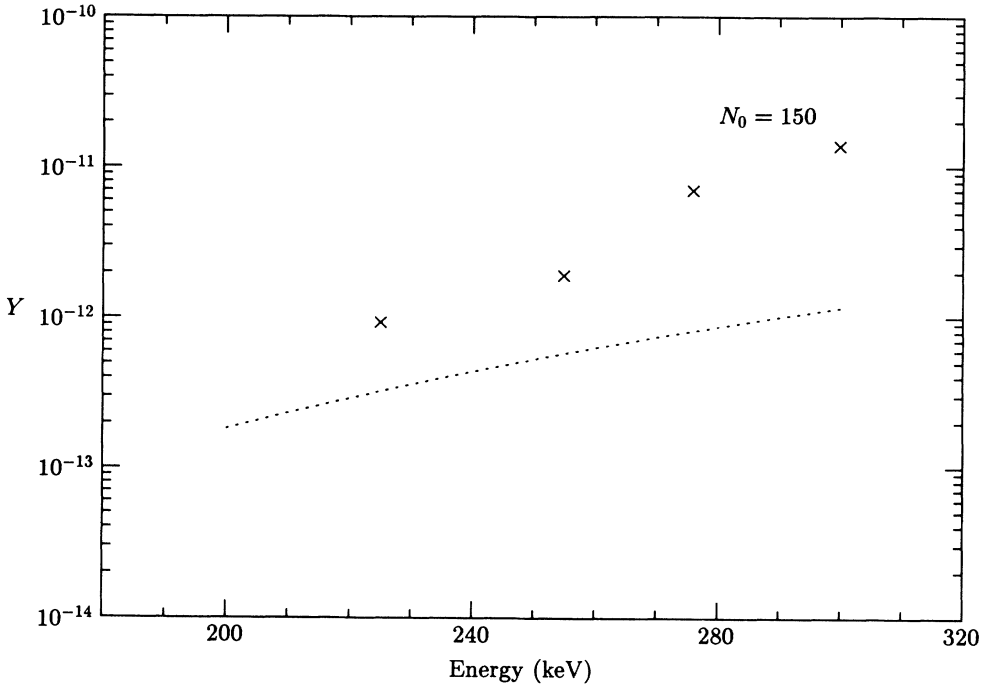

FIG. 4. Thick-target fusion yield (Y_{TT}) as a function of laboratory energy for a Gaussian distribution of cluster size centered around $N_0=150$ [see Eq. (26) with $\alpha=0.5$]. The experimental points are taken from Fig. 4 of Ref. 1 and normalized as described for Fig. 1.

the puzzling features of the experimental data that we have discussed in the previous sections.

A. Model and numerical method

Deuterated polyethylene (CD_2) has the stoichiometry of heavy water, so that we can, with high confidence, simplify our simulation by treating the impact of heavy-water clusters on a heavy-water target. Also, we chose D_2O (rather than TiD) targets to maximize any effect of local heating through the higher stopping power. Thus, we consider a system of oxygen and deuterium nuclei with numbers in the ratio of 1:2 with the Hamiltonian

$$\mathcal{H}=\sum_i \frac{\mathbf{p}_i^2}{2m_i}+\sum_{j(>i)} Q_iQ_j\frac{e^2}{|\mathbf{r}_i-\mathbf{r}_j|}\exp(-|\mathbf{r}_i-\mathbf{r}_j|/a)\ . \tag{27}$$

Here we have assumed a pairwise internuclear interaction in the form of a screened repulsive Coulomb potential; the nuclear charges Q_i are, respectively, 1 and 8 for the deuterium or oxygen nuclei. The screening length, a, is taken to be 0.5 Å, which is purposely rather large so as to increase the interatomic cross section, and hence, the rate at which the beam deposits energy in the target. This larger screening length does not materially increase the Coulomb barrier for D+D fusion; the typical distance of closest approach between two deuterium nuclei is about 0.1 Å, so that only the prefactor in the fusion probability is affected, while the dominant Gamow factor describing Coulomb barrier penetration is unchanged. The masses m_i are 16 or 2 amu for the oxygen and deuterium atoms, respectively.

It might be objected that the Hamiltonian we have chosen does not bind the atoms into molecules. This is true, but we note that the bombarding energies (300 eV per deuteron for an $N=100$ cluster at $E_{tot}=300$ keV) are quite large compared to molecular binding energies and the impact time scales are quite short compared to the thermal breakup time of a cluster of atoms (i.e., the bombarding velocity is much greater than the thermal velocity). Thus, the attractive tail of the true interatomic potential is irrelevant and it is only important that we have properly accounted for the short-range interatomic repulsion.

Our nuclei move during the simulation in accord with the usual equations of motion. We study the evolution of the system by calculating the force on each particle exerted by all others and then stepping the equations of motion in time. We use Verlet's integration algorithm:[14]

$$\mathbf{r}_{n+1}=\mathbf{r}_n+\mathbf{v}_n\Delta t+\mathbf{a}_n\Delta t^2/2\ , \tag{28a}$$

$$\mathbf{v}_{n+1}=\mathbf{v}_n+(\mathbf{a}_{n+1}+\mathbf{a}_n)\Delta t/2\ , \tag{28b}$$

where $\mathbf{r}$, $\mathbf{v}$ and $\mathbf{a}$ are, respectively, a particle's location, velocity, and acceleration, and n labels the time interval. The size of the time step, Δt, is chosen according to the cluster's incident velocity. We monitor energy conservation throughout each of our simulations and find that it is constant with a relative error smaller than 10^{-5}.

Our initial conditions correspond to the impact of a heavy-water cluster on a heavy-water target. Both of these systems are initialized separately through molecular-dynamics simulations in cubic boxes with

periodic spatial boundary conditions. The site of a box is chosen to approximately reproduce the density of heavy water. Each system is brought to thermal equilibrium at about 300 K by repeatedly scaling the velocities. The initial conditions for the impact are then generated by placing the cluster next to, but not within, the target, and boosting it with the appropriate beam velocity. We impose no spatial boundary conditions on the impact simulation, so that the asymptotic state of the system is the dispersal of all atoms. This typically occurs on a timescale of some 50 fsec.

We have simulated the impacts of clusters composed of $N=32$, 54, 80, 128, and 180 heavy-water molecules at $E_{\text{tot}}=100$ keV. Because computational requirements limit the size of targets we can simulate, we chose to run at 100-keV total energy to increase the fraction of the total energy deposited in the target for small cluster and so make it meaningful to compare the simulations for small and large cluster sizes. For each cluster size, we have performed four separate simulations corresponding to four different configurations of the target. The latter was composed of 1024 heavy-water molecules in a cubic box of side 32 Å (i.e., some 10 atomic layers). We have run each simulation until the the cluster-target system disperses; this is about the time needed for the cluster to pass through the target if there are no interactions. Anything physically significant for fusion should happen during this initial interval.

Finally, an important point needs to be made about the reliability of the information obtained through molecular-dynamics (MD) simulation. The reported experimental fusion yields for CD_2 are about 1 in 10^{10} impacts. On the other hand, we simulate only a few cluster impacts. The reason this is sufficient is that we are not simulating the fusion yield. Indeed, this is given by the velocity distribution folded into the cross section. The latter is known by quantum mechanics, and MD is concerned only with the former. Because the cross section is a rapidly increasing function of energy, the Yield is dominated by the upper end of the energy distribution.

Let the number of high-energy deuterons be $n(E_{\max})$. Then the yield per cluster is essentially [from Eq. (4)]

$$Y \sim n(E_{\max}) 10^{-6} e^{-44.24/\sqrt{E_{\max}}} \sim 10^{-10} .$$

Therefore,

$$n(E_{\max}) \sim 10^{-4} e^{44.24/\sqrt{E_{\max}}} .$$

Even if conditions were created to boost the energy of a target deuteron by, say, a factor of 40 over the initial energy of deuteron in the beam for cluster size $N=150$, one would have

$$n(E_{\max}) \approx 6 \times 10^2 .$$

Such distributions would be easily observed in a MD simulation.

We also point out that no significant difference in energy and density distribution is found between the results we present in the next section and those obtained in Ref. 3 by simulating several *thousand* cluster impacts. Finally, it is obvious from the previous discussion that main beam-energy dependence of the yield is given by the cross section, not by the velocity distribution, and this makes

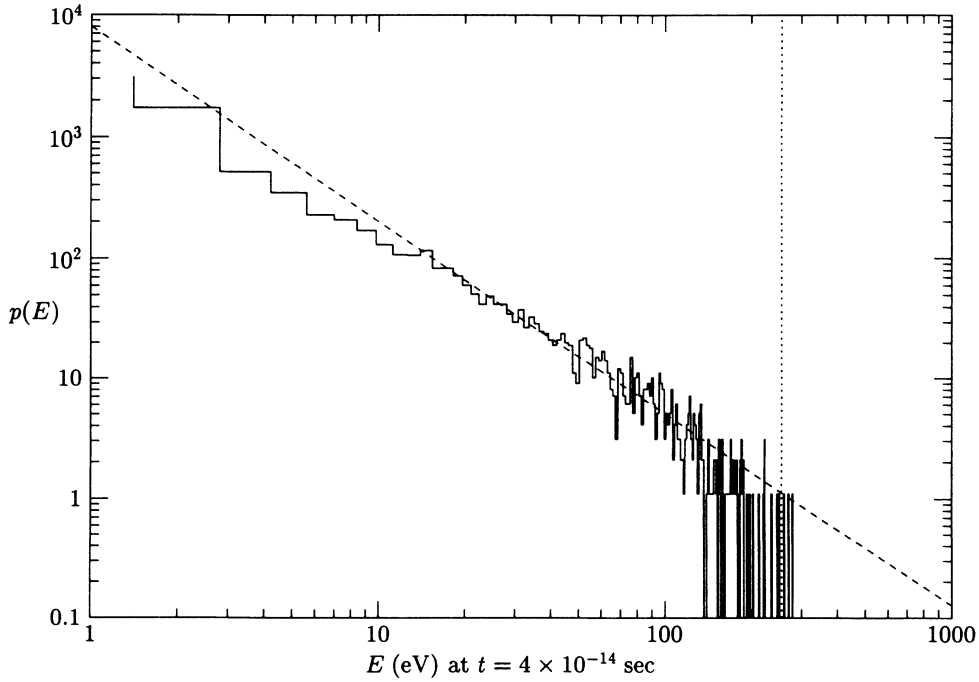

FIG. 5. Energy spectrum of target deuterons for $N=128$ at time $t=4\times10^{-14}$ sec. The dashed line shows a spectrum proportional to $E^{-1.6}$, the dotted line shows the spectrum expected from a single knock-on process. The normalization is arbitrary.

us confident in applying our 100-keV simulations to 300-keV beam-energy experiments.

B. Results and analysis

In Fig. 5 we show the energy spectrum of the *target* deuterium atoms following impact by an $N=128$ cluster. The high-energy spectrum is approximately $p(E) \propto E^{-1.6}$ consistent with experimental study and other computer simulation of sputtering yield results. It is not hard to see that the spectrum is cut off for energies greater than four times that of the incident deuterons (i.e., velocities twice that of the beam).

In Fig. 6 we show the maximum velocity of a target deuterium atom during the simulations. To meaningfully compare impacts of different size clusters, we have normalized the velocity by the beam velocity and use the (noninteracting) depth of penetration into the target as the independent variable. In all cases, at the end of the simulation, the fastest deuterium atom belonged to the target initially, as is expected form the knock-on process described in Sec. II B. The maximum deuterium velocity never exceeds twice that of the beam, which is about the maximum speed that can result from a single knock-on. Comparing the five curves corresponding to the five different cluster sizes, we can see that $V_{\max}/V_{\text{beam}}$ increase very slowly with N. This is because, with the increasing cluster size, the collision probability between beam and target atoms increases and thus there is a greater likelihood of a knock-on with large energy transfer. However, even as N changes from 32 to 180, the maximum velocity relative to beam velocity increases by only 10–15 %.

In Fig. 7 we show the maximum local deuterium densities attained during the various simulations as a function of penetration depth. These correspond to an average over a cubic box of side 5 Å. It can be seen that the highest compressions occur early in the simulation and that the maximum local density is about five times the initial density; this is far too small to enhance the fusion rates by the amount required.

We have also analyzed the distances of closest approach for pairs of deuterium atoms during the simulations. We found that the closest a pair *ever* approached each other was 0.0847 Å for $N=32$ impacts and 0.1605 Å for $N=180$ impacts. Assuming vanishing impact parameter, these distances correspond to relative kinetic energies of 143 and 65 eV, respectively. Although it is difficult to extract a meaningful fusion yield from our data, it is clear that the yield will drop very rapidly with increasing cluster size.

V. SUMMARY

In summary, we have analyzed several different mechanisms that could lead to fusion when heavy-water molecular clusters impact deuterated targets. We first considered the thick-target yield (Sec. II A); i.e., the fusion yield expected assuming that cooperative effects, such as heating, compression, or fluid-dynamic tamping, are unimportant, at least on the time scale relevant to fusion. This estimate is certainly appropriate if high-energy deuteron contaminants are present in the beam. We have elucidated the importance of careful beam analysis to prevent both high-energy contamination and mass disper-

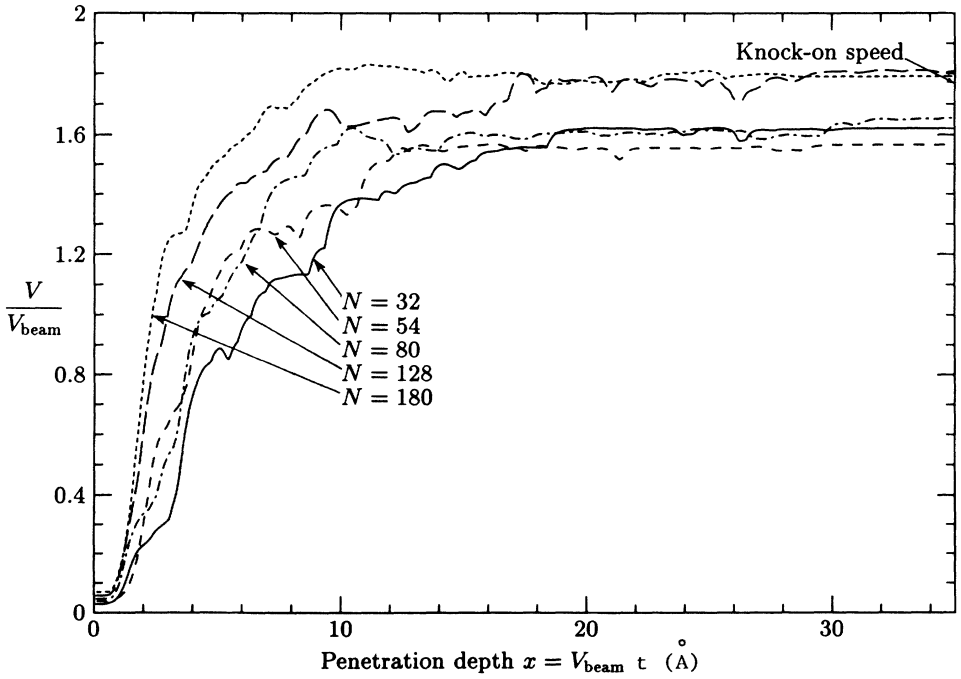

FIG. 6. Maximum target deuteron velocity normalized to the beam velocity as a function of penetration depth of the beam.

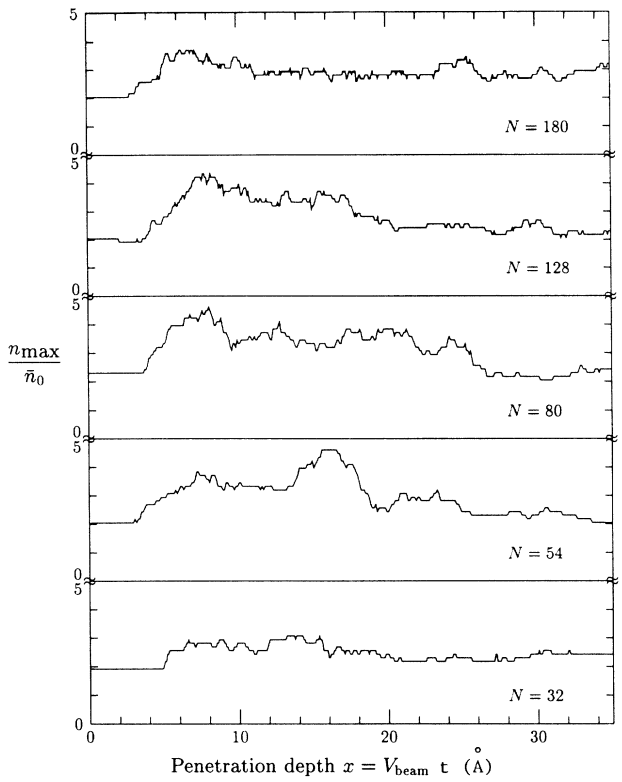

FIG. 7. Maximum local deuteron density, normalized to the initial deuteron density average, inside a cubic box of side 5 Å as a function of penetration depth of the beam; $E_{tot} = 100$ keV.

sion of the beam (Sec. III).

The simplest mechanism beyond the thick-target yield is knock-on of deuterons by heavy atoms in the incident cluster. We calculated the yield expected if only the first knock-on process is important, and subsequently refined the estimate to include multiple knock-on events (Secs. II B and II C). We point out that a knock-on yield is expected regardless of the isotopic composition of the cluster hydrogen.

Should local heating and/or compression be important, they are best described by the thermal-spike model we considered (Sec. II E). The thermonuclear model we also treated perhaps overemphasizes the effect of confinement of a hot plasma in the target (Sec. II D). The assumption of thermalization inherent in both models is appealing for several reasons,[11] not least because it allows an analytic calculation. Unfortunately, thermalization is known to be a poor description of single-molecule impacts, for example, as shown by molecular-dynamics simulations of sputtering processes.[13] We have therefore also considered the cluster fusion yield expected in light of the well-established results for ion-beam sputtering; this essentially recovers the knock-on yields (Sec. II F). We believe that these latter estimates (or those of the thick-target model, whichever is dominant) are the most realistic expectations for cluster fusion experiments.

Each of the theoretical models we have considered embodies a different intuition about fusion during cluster impact, while at the same time allowing estimates to be made by straightforward algebra. Nevertheless, the only "assumption-free" estimate of cluster-impact fusion yields can come from molecular-dynamics simulations (if one is willing to accept Newtonian mechanics and standard nuclear reaction rates). We have performed such simulations (Sec. IV). We found that no deuterium atom ever moves more rapidly than about twice the velocity of the incident cluster, that the relative energies of deuterium-deuterium collisions decline significantly with increasing cluster size at fixed total energy, and that compressions no higher than fivefold are achieved during cluster impact. These results imply that the D+D fusion yield from cluster impacts will be no larger than the knock-on yields predicted in Sec. II B and that the yield will decline precipitously with increasing cluster size. Both of these conclusions are in contradiction with the experiments reported in Ref. 1.

ACKNOWLEDGMENTS

This work has been supported in part by the National Science Foundation, Grant Nos. PHY86-04197 and PHY88-17296. We are grateful to the authors of Ref. 1 for their frank discussions and for conversations with C. A. Barnes and T. A. Tombrello. We acknowledge a time allocation on the JPL/Caltech Cray X-MP/18.

[1]R. J. Beuhler, G. Friedlander, and L. Friedman, Phys. Rev. Lett. **63**, 1292 (1989).

[2]R. J. Beuhler, G. Friedlander, and L. Friedman (private communication).

[3]T. A. Tombrello (private communication); M. H. Shapiro and T. A. Tombrello, Phys. Rev. Lett. (to be published).

[4]D. D. Clayton, *Principles of Stellar Evolution and Nucleosynthesis* (McGraw-Hill, New York, 1968), Chap. 3.

[5]W. A. Fowler, G. R. Caughlin, and B. A. Zimmerman, Annu. Rev. Astron. Astrophys. **5**, 525 (1967).

[6]At the highest energy we consider, $E_{c.m} = 150$ keV, one has $S(E)/S(0) \sim 1.3$.

[7]H. H. Andersen and J. F. Ziegler, *Hydrogen Stopping Powers and Ranges in All Elements* (Pergamon, New York, 1977).

[8]P. D. Townsend, J. C. Kelly, and N. E. W. Hartley, *Ion Implantation, Sputtering and Their Applications* (Academic, London, 1976), pp. 19–21.

[9]E. Fermi, Phys. Rev. **75**, 1169 (1949).

[10]J. C. Solem (private communication).

[11]P. Sigmund and C. Claussen, J. Appl. Phys. **52**, 990 (1981).

[12]M. W. Thompson, Philos. Mag. **18**, 377 (1968).

[13]B. J. Garrison, Nucl. Instrum. Methods **B40**, 313 (1989), and references therein.

[14]L. Verlet, Phys. Rev. **159**, 98 (1967).